UCRL-JRNL-216716

LAWRENCE
LIVERMORE
NATIONAL
LABORATORY

On the control of filamentation of intense laser beams propagating in underdense plasma

E. A. Williams

November 1, 2005

Physics of Plasmas

This document was prepared as an account of work sponsored by an agency of the United States Government. Neither the United States Government nor the University of California nor any of their employees, makes any warranty, express or implied, or assumes any legal liability or responsibility for the accuracy, completeness, or usefulness of any information, apparatus, product, or process disclosed, or represents that its use would not infringe privately owned rights. Reference herein to any specific commercial product, process, or service by trade name, trademark, manufacturer, or otherwise, does not necessarily constitute or imply its endorsement, recommendation, or favoring by the United States Government or the University of California. The views and opinions of authors expressed herein do not necessarily state or reflect those of the United States Government or the University of California, and shall not be used for advertising or product endorsement purposes.

Updated October 14, 2003

On the control of filamentation of intense laser beams propagating in underdense plasma

E. A. Williams

Lawrence Livermore National Laboratory,

University of California

Livermore, California 94550

(Dated: October 27, 2005)

Abstract

In indirect drive ICF ignition designs, the laser energy is delivered into the hohlraum through the laser entrance holes (LEH), which are sized as small as practicable to minimize X-ray radiation losses. On the other hand, deleterious laser plasma processes, such as filamentation and stimulated back-scatter, typically increase with laser intensity. Ideally, therefore, the laser spot shape should be a close fit to the LEH, with uniform (envelope) intensity in the spot and minimal energy at larger radii spilling onto the LEH material. This keeps the laser intensity as low as possible consistent with the area of the LEH aperture and the power requirements of the design. This can be achieved (at least for apertures significantly larger than the laser's aberrated focal spot) by the use of custom-designed phase plates. However, outfitting the 192 beam (National Ignition facility) NIF laser with multiple sets of phase plates optimized for a variety of different LEH aperture sizes is an expensive proposition. It is thus important to assess the impact on laser-plasma interaction processes of using phase plates with a smaller than optimum focal spot (or even no phase plates at all!) and then de-focussing the beam to expand it to fill the LEH and lower its intensity. We find significant effects from the lack of uniformity of the laser envelope out of the focal plane, from changes in the characteristic sizes of the laser speckle, and on the efficacy of additional polarization and/or SSD beam smoothing. We quantify these effects with analytic estimates and simulations using our laser plasma interaction code pF3D.

PACS numbers: 52.40.Nk, 52.35Mw, 52.65.Rr

I. INTRODUCTION

When a high powered laser beam passes through a plasma, it is potentially subject to a variety of instabilities which can scatter and absorb the light. [1, 2] Stimulated Brillouin (SBS) and stimulated Raman (SRS) scattering respectively scatter the incident light from ion acoustic and Langmuir waves parametrically excited in the plasma medium.

Filamentation[3] and self-focusing[4] are processes in which transverse variations in the laser intensity are amplified on passage through the plasma. The filamentation moniker is applied to the linear instability of plane wave pumps in which modulations grow from small initial perturbations, whereas self-focusing refers to the contraction and intensification of the whole laser beam. The underlying physics is the same. The major difference is that in the case of filamentation, the transverse scale is picked by the maximum of the growth rate, whereas for self-focusing the spatial scales derive more from the initial conditions. In this paper, we will be concerned with laser beams that are highly aberrated and/or have been processed by phase plates. [5, 6] The transverse intensity profile of such beams has small scale, large amplitude intensity fluctuations (speckles), modulating the large scale (envelope) intensity profile of the entire beam cross section. In such beams, the filamentation process can act on both scales, causing the higher intensity speckles to self focus and spray light to larger angles, and on a longer time and space scale the entire beam to channel and self-focus.

In indirect drive inertial confinement fusion (ICF), x-ray radiation is created by illuminating the inside wall of a cylindrical hohlraum with lasers focused through an entrance hole (LEH) in the ends.[7–9] The x-rays in turn ablate and implode a spherical capsule filled with DT placed at the center of the hohlraum. Since X-ray power is lost through the LEH proportionate to its area, energetic optimizations drive designs to minimize the LEH area. However, this is in direct conflict with the desire to minimize laser scattering instabilities which increase with laser intensity.

In this paper we consider the question of how to deliver a given laser power through a given size aperture to minimize deleterious laser plasma interactions.

II. PHASE PLATES.

Phase plates are optical elements placed in the laser beam path that introduce an optical phase shift that varies across the beam. The simplest form, a random phase plate (RPP), consists of a regular array of identical elements, each of which either introduces, at random, either a zero or pi phase shift. We briefly review their theory of operation here.

Consider for definiteness, a plane wave laser beam incident on a square RPP with side a, which consists of N^2 square elements with side a/N. The beam is brought to a focus by a lens of focal length F. Each element independently gives rise to a focal spot with transverse dimension $NF\lambda_0/a$, where λ_0 is the laser wavelength. The profile of the focal spot is the diffraction pattern of the phase plate element, in this case the Fourier transform of a square. The depth of focus of a beamlet, $(NF/a)^2\lambda_0$, is larger than the distance over which the beamlets de-overlap $N(F/a)^2\lambda_0$, so for large N, we can ignore the effect of diffraction on the individual beamlets as we move out of the focal plane. The laser electric field $E(\mathbf{x}, z)$ in the vicinity of the focal point thus takes the form of the sum of enveloped plane waves

$$\mathbf{E}(\mathbf{x}, z) = \Sigma_i A(\mathbf{x} - \mathbf{y_i} z/F, z) \exp(i\mathbf{x} \cdot \mathbf{y_i} k_0/F - i y_i^2 k_0 z/2F^2 + i\phi_i) \tag{1}$$

Here $(\mathbf{x}, z)$ are spatial coordinates relative to focus, with z the propagation direction. The sum is over the coordinates y_i of the phase plate elements, whose phase shifts are ϕ_i. The laser has wavenumber k_0 and propagates in the z-direction. The envelope function $A(\mathbf{x}, z)$ is the Fourier transform of the element aperture function.

At any fixed point inside the focal spot the laser field is seen to be the sum of a large number of contributions with random relative phases. The real and imaginary parts are independently Gaussian distributed with zero mean, by the central limit theorem, and the intensity is thus exponentially distributed with a mean given by the local envelope intensity $\Sigma_i |A(\mathbf{x} - \mathbf{y_i} z/F, z)|^2$. [10–12]

Displacements of $\mathbf{x}$ or z shift the relative phases in the exponential in Eq. (1), decorrelating the intensity over distances $|\delta\mathbf{x}| \simeq f\lambda_0$ or $\delta z \simeq 2f^2\lambda_0$, where $\lambda_0 = 2\pi/k_0$ and the f-number f is given by $f = a/F$. The typical speckle size is thus given by the diffraction limit of the entire optic, whereas the spot size is that of a single phase plate element.

More sophisticated phase plate designs (e.g. continuous and kineform phase plates CPP/KPP) [13, 14] use a smoothly varying "random" phase. By removing the discontinuities in the phase one can create far fields that throw less energy outside of the main focal

spot. One can readily obtain a similar expression for the far field to Eq. (1). The sum over phase plate elements is replaced by a sum over the points in the the near field where the normal to the constant phase surface is directed at the point $(\mathbf{x}, z)$ in the far field.

Nova was equipped with phase plates designed to create super-Gaussian elliptical spot shapes. Corresponding designs have been prototyped for the National Ignition Facility (NIF) laser. The spot shape is elliptical in order to fit the LEH at oblique incidence.

A useful measure of the intensity distribution of a laser spot is the fraction of the laser power that is above a specified intensity (FOPAI). For a flat topped enveloped RPP, this given by the expression $(1 + I/\bar{I}) \exp(-I/\bar{I})$, where $\bar{I}$ is the envelope intensity. For a non-uniform envelope, this expression has to be convolved with distribution of $\bar{I}$. Perhaps surprisingly, the FOPAI distributions of *unsmoothed* (no phase plate) Nova and NIF at various distances from focus are quite similar to that of phase plate beams, with an appropriate choice of $\bar{I}$. This results from the phase aberrations of these beams varying rapidly and quasi randomly across the near field cross section, causing the far field to be the sum of numerous contributions. Note that the much of the phase aberration in these high power lasers arise from nonlinear optical effects in the glass, not just from the classical effects like spherical aberration, astigmatism etc, which are less random in character.

In Fig. 1 the FOPAI for the Nova KPP used in f/4 experiments is compared with the unsmoothed Nova beam[15] with a range of distances of defocus. All beams have the same power, and the intensity is expressed in terms of the nominal intensity, that is the power divided by the area of the 95% power ellipse. First we note that the the KPP curves lies slightly above that of the analytical curve. This is is primarily because of the Nova beam aberrations.

To fit 95% of the beam power through the same nominal ellipse of the KPP beam, it was necessary to defocus the unsmoothed Nova by 1.1 mm. The resulting FOPAI has significantly more power at high intensity, corresponding to a nominal intensity 1.7 times higher. Alternatively, in order to match the FOPAI distribution of the KPP, one needed to defocus by 1.5mm, which would have resulted in 12% of the power outside the nominal spot.

Matching FOPAI curves gives us a sensible way of comparing the intensities of two beams, given that power divided by spot size is such an ill-defined measure when you have an unsmoothed spot like we illustrate in Fig. 2.

We consider two FOPAI curves to be equivalent if the areas under them are equal. This is equivalent to requiring the power-weighted intensities, given by $I_p \equiv \int I^2 dA / \int I dA$ be equal. We will discuss additional theoretical grounds for this particular choice shortly. However, there are other sensible choices. A possible one would be matching the curves at, say, the 5% power point, if one was especially concerned when 5% of the incident power exceeded some local intensity threshold in the plasma. In the cases discussed here, the differences are not significant.

The FOPAI is clearly significant for intensity dependent plasma processes that are localized to the speckle size, such as speckle self-focussing and parametric stimulated scattering when the length of the resonance region does not significantly exceed the length of the speckle. In this situation an independent speckle model is appropriate and an integration over the beam cross-section becomes one over the speckle intensity distribution. [16–18]

Moreover, in the opposite limit, where the parametric gain region extends over many ranks of speckles, I_P enters the spatial growth rate.

Consider SBS or SRS in which we take the paraxial approximation for the electromagnetic waves and assume that the ion/plasma wave is strongly damped (spatial damping rate exceeding the spatial amplification rate of the instability). If we further assume a steady state is reached, then the scattered power P_1 satisfies an equation of the form

$$\frac{\partial P_1}{\partial z} = -\int d^2x_\perp g I_0 I_1 \tag{2}$$

where the power $P_i = \int d^2x_\perp I_i(x_\perp)$ is the intensity of the pump (I_0) and scattered light (I_1) integrated over the beam cross-section. If, for tractability, we also neglect the transverse variation of the spatial gain coefficient, we see that the effective pump intensity is one weighted by the scattered light intensity, that is

$$\frac{\partial P_1}{\partial z} = -g\bar{I}_0 P_1 \tag{3}$$

with

$$\bar{I}_0 = \int d^2x_\perp I_0 I_1 / \int d^2x_\perp I_1 \tag{4}$$

The scattered mode with the largest amplification is thus the one that maximizes the overlap of the pump and scattered intensities over the entire gain region. For SBS backscatter, under certain conditions (no pump depletion, gain per speckle not large, this will be the phase conjugate mode [19], when $I_1 \propto I_0$ and the beams overlap speckle by speckle.

In this case $\bar{I}_0 = I_P =< I_0^2 > / < I_0 >$. For a flat-topped RPP speckle distribution this gives a well-known factor of two increase of total gain over that computed from the average intensity. [20]

For SRS, because of the large wavelength difference with the pump, modes cannot overlap speckle for speckle over multiple speckle lengths. The same is true for non-conjugate SBS. In this case, matching the *envelope* intensities of the pump and scattered waves gives $\bar{I}_0 = I_P/2$.

In all these cases I_P is an appropriate parameter for comparing two pumps with different distributions of intensity.

However, the lower I_P of a beam produced by a phase plate compared with an unsmoothed beam defocussed to the same power through the phase plate's spot is not the only significant difference between them. The speckle size of the defocussed spot is generally larger.

III. SPECKLE SIZE

In the focal plane ($z = 0$) of a beam spatially smoothed by a random phase plate, we argued in section II that the transverse dimension of a typical speckle is approximately $f\lambda_0$. As we move out of focus, we see from Eq. (1), and illustrated in Fig. 3, that the contributions from the individual phase plate elements cease to overlap. In the figure we depict an ideal nine element square phase plate that generates an envelope intensity that is constant inside a disk and zero outside. Starting at the edge of the spot and working inward as z increases, the intensity drops, being proportional to the number of phase elements elements contributing to it. At the same time, where the intensity drops, the speckle size increases, because the angular size of the contributing part of the beam aperture decreases. We can see this more formally by considering the Fourier transform of the electric field auto-correlation function, which is given by

$$\int d^2X \langle E(\mathbf{x}+\mathbf{X},z)E^*(\mathbf{x},z)\rangle \exp(i\mathbf{k}\cdot\mathbf{X}) \propto |A(\mathbf{x}-\mathbf{k}z/k_0)|^2 S(F\mathbf{k}/k_0) \tag{5}$$

where $S(\mathbf{y})$ is the near field intensity across the phase plate. In the ideal case of the disk envelope, the $|A|^2$ factor is zero or one depending on whether the phase plate element in the direction of $\mathbf{k}$ contribute in the neighborhood of the point $(\mathbf{x}, z)$ in the far field. To first approximation then, the speckle area goes inversely as the intensity and the product, the power per speckle remains constant as one moves out of focus. Phrased another way,

the number of speckles, (beam power divided by power per speckle) ill-defined as that is, remains constant as the beam propagates.

This is of particular significance for speckle self-focusing, whose threshold is determined by the laser power per speckle as we shall discuss shortly.

We can conveniently make a global definition of speckle area, $(f_{eff}\lambda_0)^2$, with f_{eff}, an effective f-number in the following fashion:

$$(f_{eff}\lambda_0)^2 \equiv C \int d^2x I(\mathbf{x})^2 / \int d^2x |\nabla I(\mathbf{x})|^2 \tag{6}$$

where we can choose the constant C so that f_{eff} is the lens f-number when the beam is smoothed by an ideal flat-topped envelope phase plate.

In Fig. 4, we plot f_{eff} vs. distance of defocus for an unsmoothed Nova beam and for the same beam smoothed by a Nova phase plate. We see that at 1.1 mm defocus, where the unsmoothed beam had the same nominal intensity (power/area of 95% power ellipse) as the KPP smoothed beam at focus, the effective f-number, $f_{eff} \simeq 13$, is substantially greater than the KPP beam's f/4.7. As the beam expands from best focus, the speckles expand with it.

IV. SPECKLE SELF-FOCUSING AND CRITICAL POWER

Laser light propagating through plasma is subject to the well-known filamentation instability. In one manifestation, plane waves are subject to breakup into filaments by the amplification of transverse perturbations. In another, whole beams self focus, or not, according whether the power in the beam exceeds a critical power that depends on plasma conditions. We are concerned here with the self focusing of speckle structure within a beam. There is a body of analytic and simulation work on the interaction of RPP smoothed beams with plasma. [21–25] Nevertheless, it is worthwhile to show here a simple argument to show that power per speckle is the important parameter to characterize the beam, independent of the specfic self-focusing mechanism. Consider the propagation of a particular speckle in the plasma. Expanding around the maximum, we can write the intensity as

$$I(x) = I_0(1 - x^2/L^2) \tag{7}$$

The high intensity drives a electron density perturbation $n(x)$ of the form:

$$n(x) = n_0(1 - \alpha I(x)) \tag{8}$$

where the coefficient α depends on the plasma conditions and the self focusing mechanism.[3, 26–30] For ponderomotive filamentation

$$\alpha I_0 = v_0^2/2v_e^2 \tag{9}$$

where v_0 is the oscillatory velocity of an electron in the laser field with intensity I_0, and v_e is the electron thermal velocity.

If we consider a light ray traveling in the z-direction offset x from the intensity peak, the ray-tracing equation $d^2x/dz^2 = -(1/2)\nabla(n/n_c)$ becomes

$$\frac{d^2x}{dz^2} + \frac{1}{2}\frac{v_0^2}{v_e^2}\frac{n_0}{n_c}x = 0 \tag{10}$$

Each parallel ray therefore comes to a common focus after a distance $z_f = (\pi/2)(v_e/v_0)(n_c/n_0)^{1/2}L$, in the ponderomotive case. Countering this focusing tendency, the intensity inhomogeneity will diffract in a characteristic distance $z_d = L^2/\lambda_0$, where λ_0 is the laser wavelength. A given speckle can therefore be expected to self focus if $z_f < z_d$, or neglecting numerical factors $(v_0/v_e)^2(n_0/n_c)(L/\lambda_0)^2 > 1$. We can write this in the form $I_0L^2 >$ some function of plasma conditions. This would be the case for any self-focusing mechanism in which the density response is linear in the laser intensity. It is therefore clear that for any such mechanism, the dependence on the laser field is entirely through I_0L^2, the power per speckle.

Using I_P, the power-averaged intensity, to characterize the distribution of speckle intensities and f_{eff}^2 to characterize the speckle area, we can use $I_Pf_{eff}^2$ to compare the effect of different laser focussing and spatial smoothing schemes on speckle self-focusing for any given set of plasma conditions.

In Fig. 5 we plot $I_Pf_{eff}^2$ versus defocusing distance for the Nova KPP and unsmoothed beams. Experiments on Nova using unsmoothed beams typically used 1-2 mm of defocus. KPP smoothed beams were used at their focus. Because of the increase in f_{eff} from defocus and the inhomogeneous envelope of the unsmoothed beam, we see that the speckle self-focusing tendency of the unsmoothed beam was some 12 times higher than the nominally equivalent KPP beam. It is therefore not surprising, in retrospect, that phase plates had such a dramatic effect on laser plasma interactions, reducing beam bending [31, 32], backscatter and increasing hohlraum radiation temperatures.[7, 33, 34] Simulations comparing smoothed and unsmoothed Nova beams showed dramatic differences in propagation. [24] Note that for

the KPP, the power per speckle is almost independent of defocus, as anticipated above, and that the same is true for the unsmoothed beam beyond approximately 0.5 mm of defocus, indicating the the beam aberrations approximate a poor quality phase plate.

V. NIF BEAMS.

The NIF laser is designed to have 192 beams, arranged in closely packed groups of four, referred to as quads. The four beams of a quad share a common beam port on the target chamber. Each beam has a rectangular aperture and is independently pointable and focusable. This provides a benefit not available in earlier lasers like Nova and Omega. If the four beams are defocused and pointed so that beams fully overlap, then with or without phase plates, each point in the far field will have contributions from the near field of all four beams. The speckle structure size will thus be determined by the inter-beam interference, not by the f_{eff} of the individual beams, and thus does not significantly increase with defocus.

This is illustrated in Figs. 6-7, where we show the contributing portion of the near field (i.e. the contributing phase plate elements) at a point in the penumbra of an 842 by 632 μm KPP smoothed beam defocussed 3.8 cm to a 1 mm by 806 μm spot. (It is worth mentioning here, that in this penumbral region of the spot, SSD loses effectiveness, because the total instantaneous bandwidth decreases with decreases in the visible aperture in the direction of SSD dispersion. [35] The polarization smoothing scheme currently envisaged for NIF, where two of the four beams of the quad would operated with crossed polarization to the remaining two would not suffer from this defect provided the beams were overlapped. [36])

In Figs. 8-9, we show a portion of the far field for an unsmoothed single member of a quad defocussed 2.2 cm and the same portion when all four unsmoothed beams are present and pointed to overlap. Here it is quite dramatic how the large scale structure of the individual beams is broken up into ∼f/8 speckles by the inter-beam interference.

One might be skeptical, however, that the regular pattern of speckles we see in Fig. 9 is equivalent for the standpoint of susceptibility to speckle self focusing, to a much more random pattern of speckles that would arise from a full f/8 aperture phase plate. That is the subject of the simulations described in the next section.

VI. SIMULATIONS WITH PF3D.

The application to the NIF laser, described above, motivated the following series of simulations using the laser propagation code pF3D.[25, 37] In these simulations light propagates in the paraxial approximation and interacts with a nonlinear single fluid plasma model via the ponderomotive force and inverse brehmsstrahlung absorption. The models for stimulated back-scatter were not activated. The plasma was taken to be a uniform slab of fully ionized CH with an electron temperature of 3 KeV, an ion temperature of 1 KeV and an electron density one tenth of the critical density for the incident 0.351 μm light. In the first pair of simulations, the incident average intensity was 10^{15} W/cm^2 and in the second pair the intensity was doubled. Each pair of simulations consisted of one in which the incident light was from an f/8 square aperture RPP, the second from four f/40 sub-apertures RPPs, arranged in a square to produce the same value of f_{eff}, as shown in Figs. 10. This is a mockup of the situation depicted in Figs. 6 and 7 The figures show the state of the simulation at 38 ps, by which time they have reached a statistical steady state.

In Fig. 10 we show the evolution of the angular distribution of the light as it propagates through the plasma. At the lower intensity, we see that in less than 750 μm of propagation both beams have slightly expanded to an approximately circular f-cone slightly larger than the original f/8 cone. The rms spread of the beams (0.071 and 0.070 radians) differ insignificantly, and from that point on the beams would be essentially indistinguishable. During the propagation, the missing regions of the f-cone were filled in by some combination of forward SBS and filamentation.

The situation at the higher intensity in Fig. 11 is very similar, except now we are significantly above the threshold for beam spray and the 750 μm f-cone is expanded from the initial angular spread. Again the missing part of the f-cone was filled in by scattering in less than 0.5 mm of plasma.

In the higher intensity case, in addition to the beam spray, we see indications of speckle self-focusing in the FOPAI distribution as a function of propagation distance shown in Figs. 12. In both cases (f/8 and 4×f/40 incident), we see 5% of the incident power is self-focused to intensities above 3-4×10^{16} W/cm^2. Both kinds of incident beam should thus produce similar enhancements of other plasma processes (such as backscatter) from the speckle self focusing process.

VII. CONCLUSIONS

For indirect drive ICF and in other applications of high-powered lasers, one often desires to deliver a given laser power through a given aperture while minimizing beam spray and other deleterious laser plasma interactions (LPI). The use of a phase plate, designed to create a flat topped envelope intensity spot to fit the desired aperture minimizes the power-averaged intensity I_P of the spot. Other schemes, such as defocusing smaller spots, for producing the desired spot size are expected to be less favorable for LPI.

When a single unsmoothed beam is defocussed, such as on Nova, not only will I_P, in general, be larger than that from a phase plate, because the beam does not fully fill the aperture, but in addition the spatial size of intensity inhomogeneities (speckles) will be larger. We have introduced a global measure f_{eff} that characterizes this. This leads to a larger power per speckle ($\propto\ I_P f_{eff}^2$), a lowered beam power threshold for speckle self-focusing and a consequent expectation of increased deleterious LPI, as was observed in Nova experiments.

With a custom phase plate unavailable, an option is to defocus a spot created by a phase plate designed for a somewhat smaller focal spot. For a single beam, this defocusing has little effect on the beam power threshold for speckle self focusing. The intensity and speckle size in the central portion of the beam are unchanged. Whereas, near the edges, where the intensity drops, the speckle area increases in an inverse manner, such that the power per speckle is unchanged.

With multiple closely separated beams that are independently focusable and pointable, as in a NIF quad, there is some benefit in defocusing a smaller RPP spot, as the speckle size (and f_{eff}) remain approximately constant provided the beams are kept overlapped. Their power-averaged intensity decreases with defocus, albeit by a smaller factor than the by ratio of the spot sizes. In some situations, overlapped defocused unsmoothed beams might be acceptable, though the probability that at a given point in the far field, the contributions to the envelope intensity from the individual beams may not be approximately equal, partially negating the benefit of inter-beam interference (as would be the case if identical phase plates were used) would have to be assessed.

Simulations showed that when overlapping phase-plate smoothed beams of sufficient power overlap, plasma propagation fills in the angular aperture between them, making the

resulting beam equivalent to one produced by a phase plate beam covering the entire aperture.

Acknowledgments

I thank my colleagues Drs. R. Berger, L. Divol, S. Dixit, S. Glenzer, D. Hinkel, A. B. Langdon and D. Munro for their valuable insights and contributions to this work.

This work was performed under the auspices of the U.S. Department of Energy by University of California, Lawrence Livermore National Laboratory under Contract W-7405-Eng-48

FIG. 1: FOPAI distributions for the Nova KPP and defocused unsmoothed beam.

FIG. 2: Unsmoothed Nova beam intensity at 1.1 mm past best focus.

FIG. 3: Envelope intensity of an out of focus nine element phase plate. Each element creates a displaced circular focal spot.

FIG. 4: f_{eff} vs. defocus for the Nova KPP and unsmoothed beams.

FIG. 5: $I_P f_{eff}^2$ vs. defocus for the Nova KPP and unsmoothed beams.

FIG. 6: Intensity of an ideal NIF KPP creating a $842 \times 632\,\mu$m focal spot, defocused 3.8 cm to a $1000 \times 806\,\mu$m spot.

FIG. 7: Portion of the phase plate contributing to the intensity at the point X in Fig. 6.

FIG. 8: Intensity in a portion of the focal spot of a single unsmoothed NIF defocused 2.2 cm.

FIG. 9: As Fig. 8, but with all four overlapping beams of the quad contributing to the intensity.

FIG. 10: Angular distribution of laser intensity of incident light and on propagation of 175 and $750\,\mu$m through a Te=3 KeV, Ti=1 KeV CH plasma at one tenth critical density for $0.351\,\mu$m light at an intensity of 10^{15} W/cm^2. In the top row the incident light is from an f/8 full aperture phase plate. In the lower row, the light is from four f/40 sub-apertures.

FIG. 11: As in Fig. 10, but at 2×10^{15} W/cm^2

FIG. 12: The fraction of power above a given intensity (FOPAI) is plotted vs. position for the high intensity case in Fig. 11. The upper contours represent 5% of the incident power.

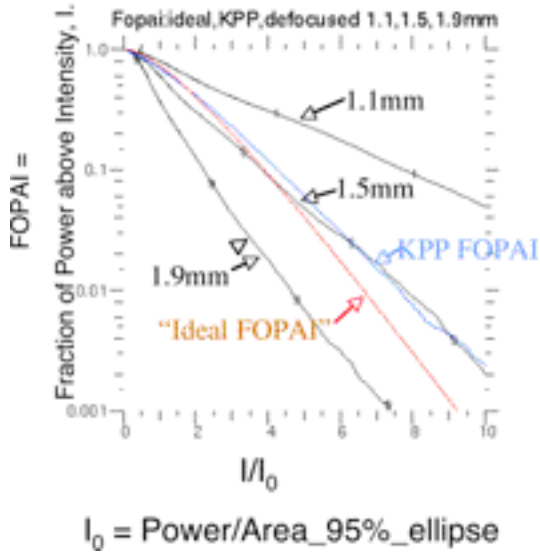

Figure 1 FOPAI distributions for the Nova KPP and defocused unsmoothed beam.

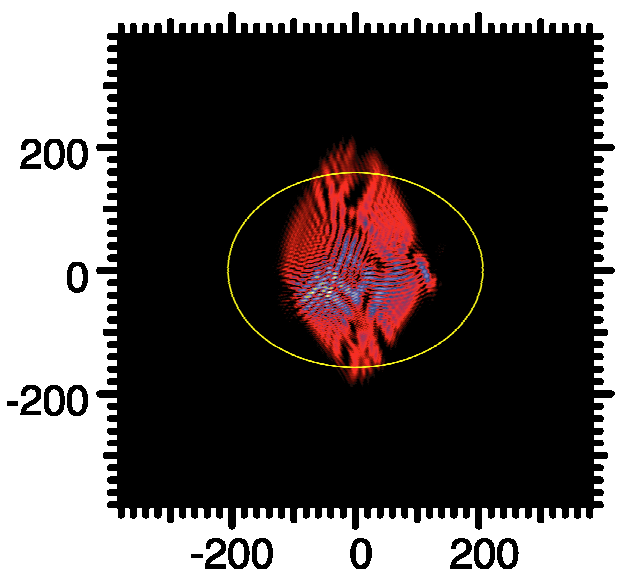

Figure 2 Unsmoothed Nova beam intensity at 1.1 mm past best focus.

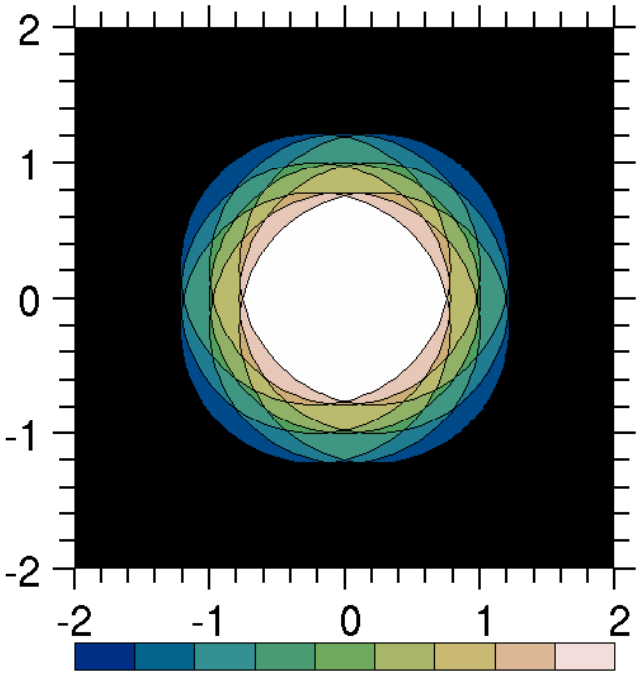

Fig 3: Envelope intensity of an out of focus nine element phase plate. Each element creates a displaced circular focal spot.

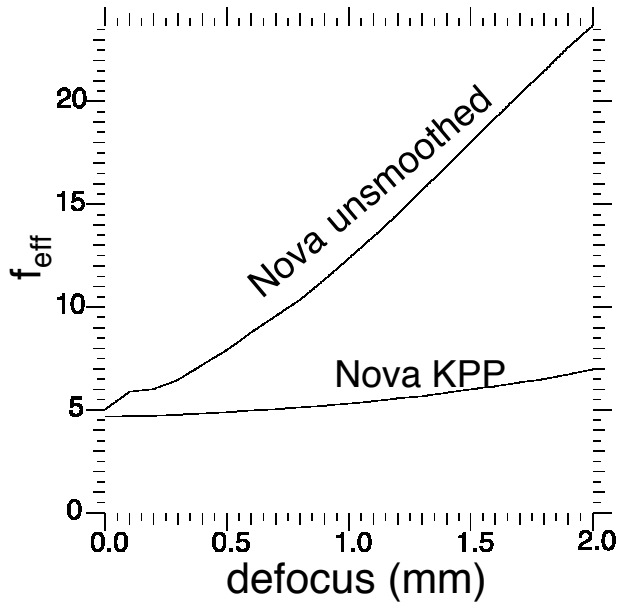

Fig:4 F_{eff} vs. defocus for the Nova KPP and unsmoothed beams.

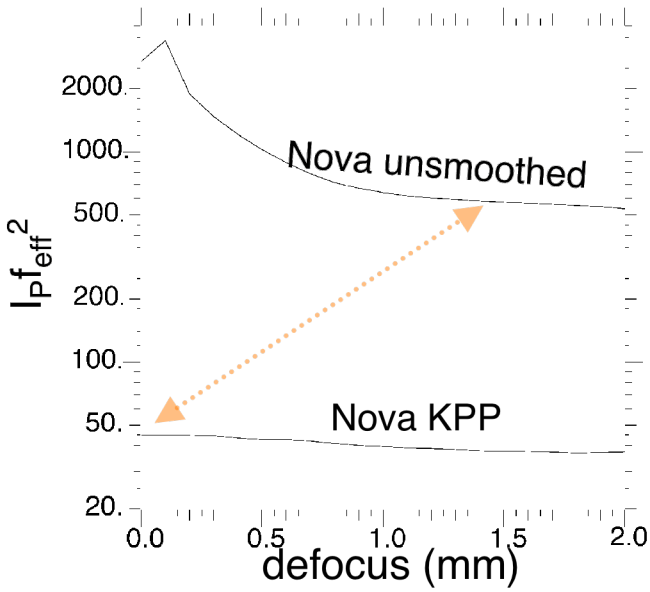

Fig 5: $I_P f_{eff}^2$ vs. defocus for the Nova KPP and unsmoothed beams.

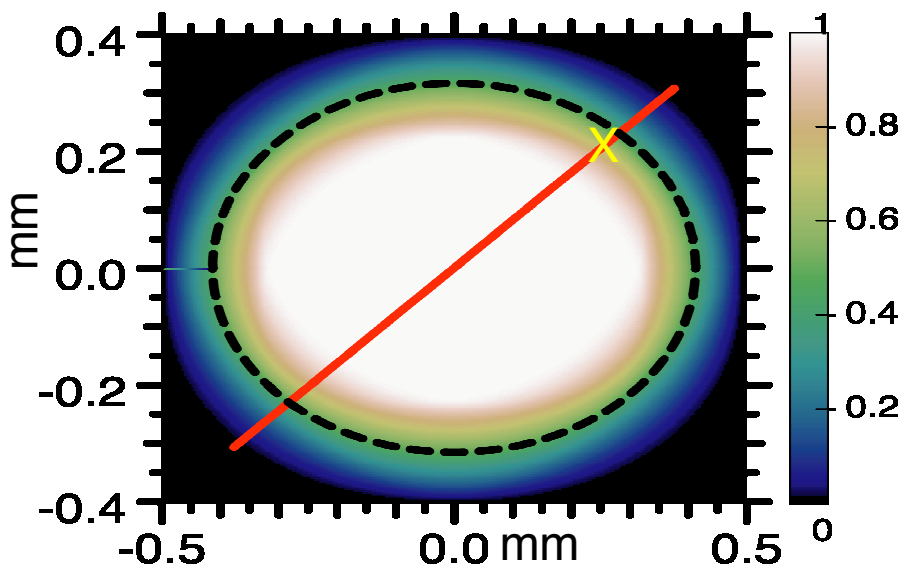

Fig 6: Intensity of an ideal NIF KPP creating a 842×632μm focal spot, defocused 3.8cm to a 1000×806μm spot.

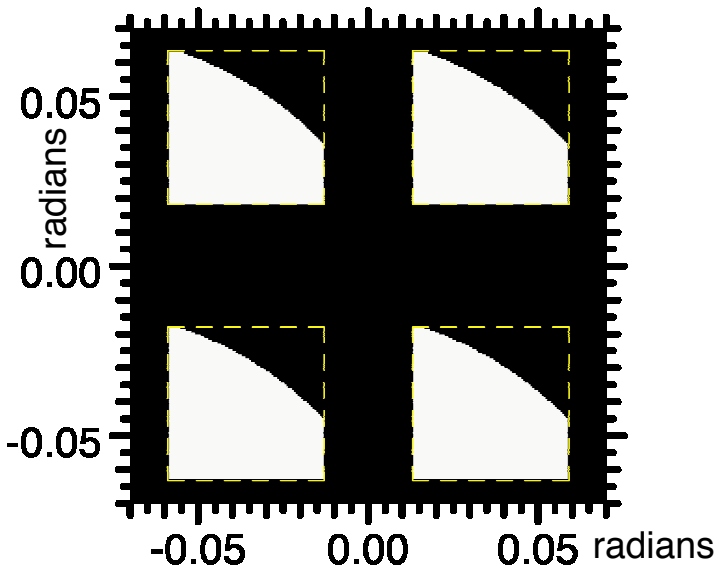

Fig 7: Portion of the phase plate contributing to the intensity at the point "X" in Fig. 6.

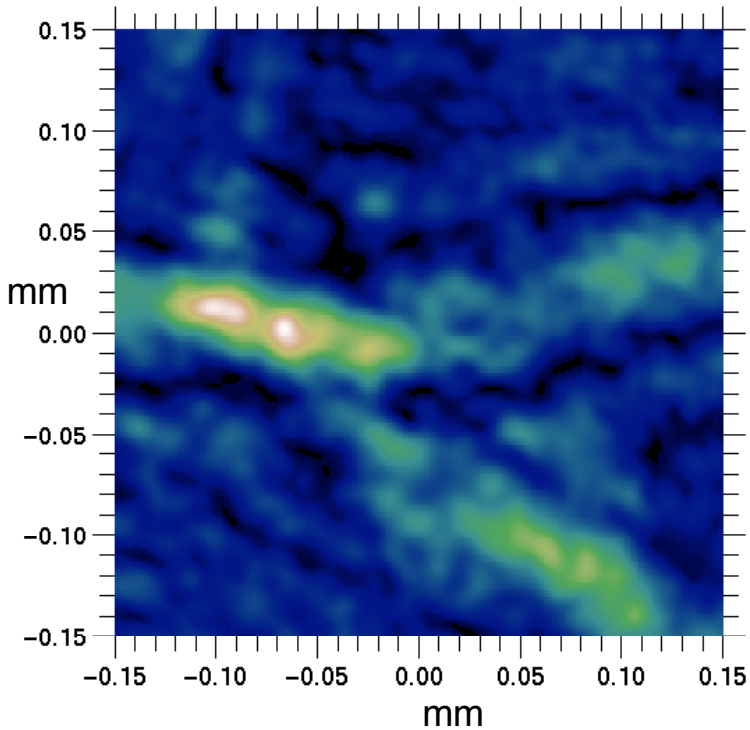

Fig 8: Intensity in a portion of the focal spot of a single unsmoothed NIF defocused 2.2 cm.

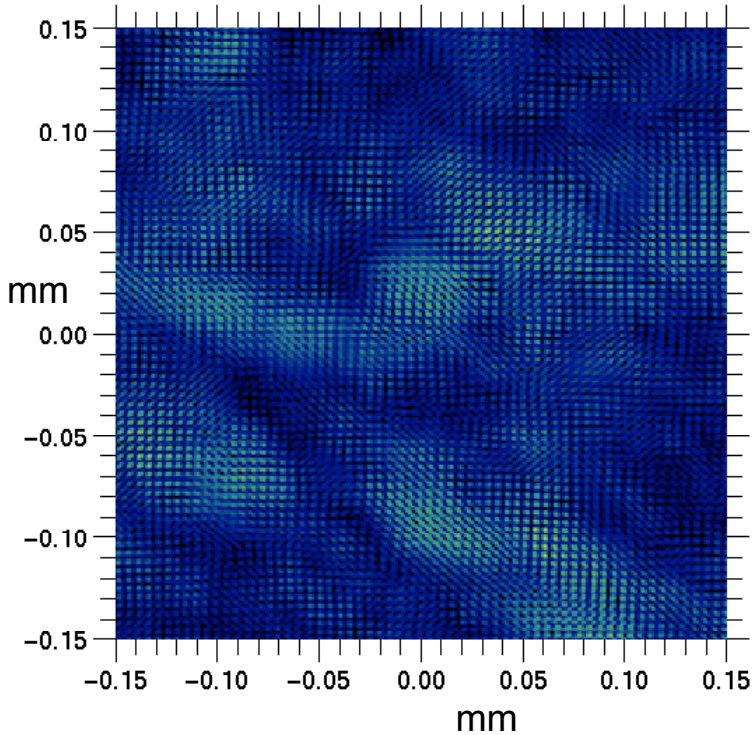

Fig 9: As Fig. 8, but with all four overlapping beams of the quad contributing to the intensity.

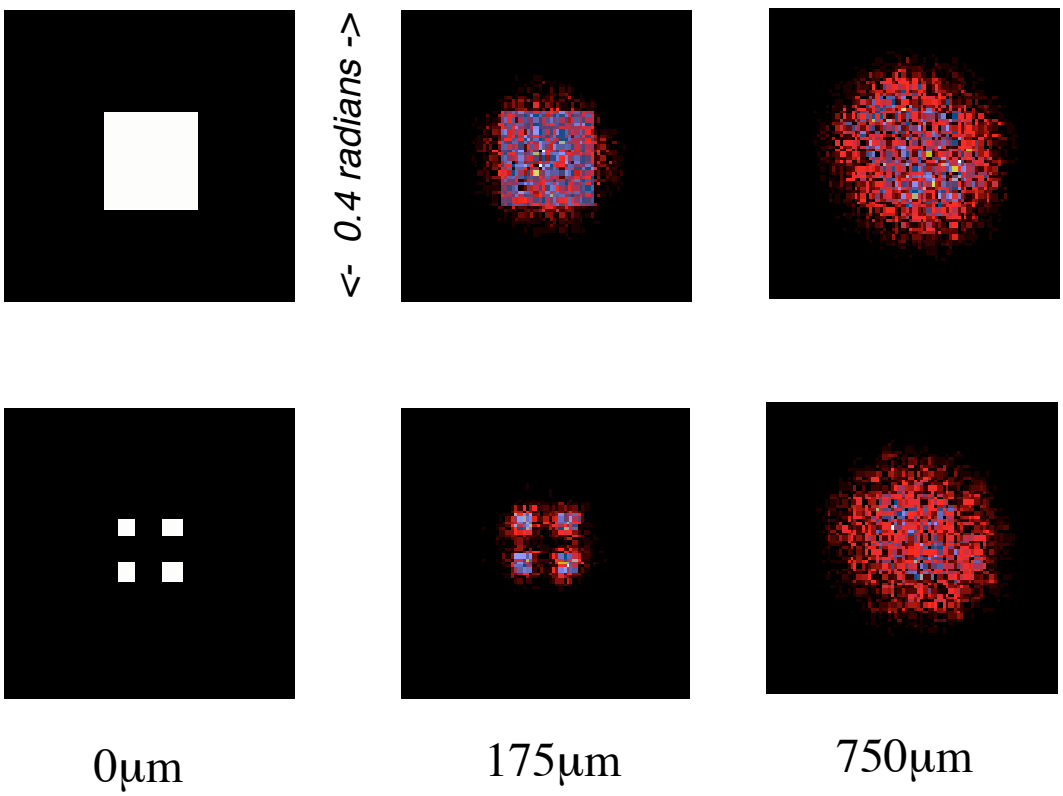

Fig 10: Angular distribution of laser intensity of incident light and on propagation of 175 and 750 μm through a Te=3 KeV, Ti=1 KeV CH plasma at one tenth critical density for 0.351 μm light at 10^{15} W/cm^2 intensity. In the top row the incident light is from an f/8 full aperture phase plate. In the lower row, the light is from four f/40 sub-apertures.

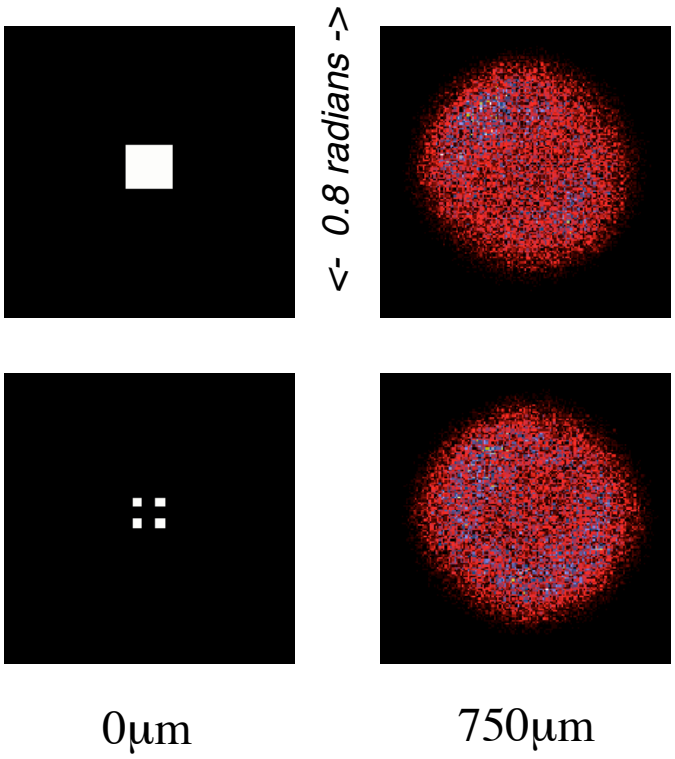

Fig 11: As Fig 10, but at 2×10^{15} W/cm^2

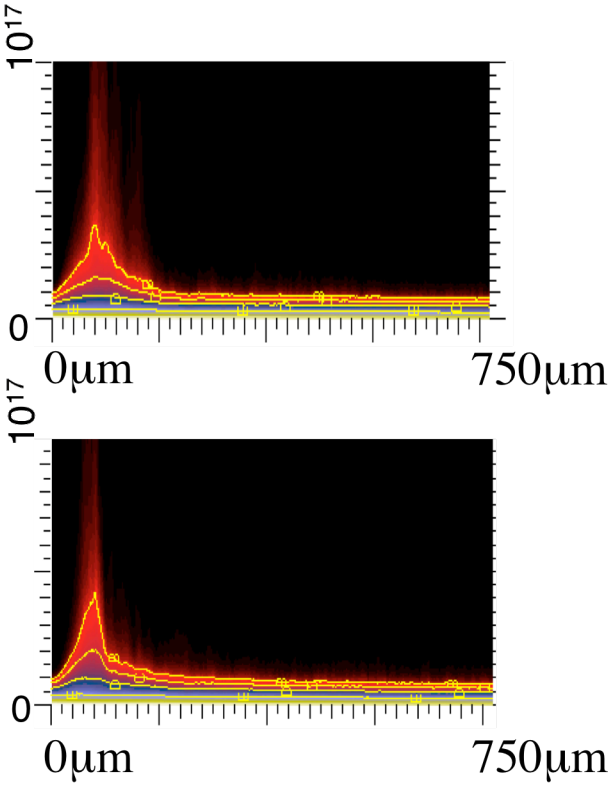

Fig 12: The fraction of power above a given intensity (FOPAI) is plotted vs. position for the high intensity case in Fig. 11. The upper contours represent 5% of the incident power.

[1] W. K. Kruer. *The Physics of Laser Plasma Interactions.* Addison–Wesley Co. Inc., New York (1990)

[2] J. F. Drake, P. K. Kaw, Y. C. Lee et. al. Phys. Fluids **17**, 778 (1973)

[3] P. K. Kaw, G. Schmidt and T. W. Wilcox, Phys. Fluids **16**,1522 (1973)

[4] C. Sulem and P. L. Sulem. *Nonlinear Schroedinger equations: Self-focusing and Wave Collapse* Springer (1999)

[5] Y. Kato and K. Mima, Appl. Phys. B **29**, 186 (1982)

[6] Y. Kato, K. Mima, N. Mivanaga et. al., Phys. Rev. Lett. **53**, 1057 (1984)

[7] J. D. Lindl et. al. Phys. Plas. **11**, 339 (2004)

[8] J. D. Lindl, Phys. Plas. **2**, 3933 (1995)

[9] S. W. Haan, S. M. Pollaine, J. D. Lindl et. al. Phys. Plas. **2**, 2480 (1995)

[10] J. Adler, *The Geometry of Random Fields*, (Wiley NY 1981)

[11] H. A. Rose and D. F. Dubois, Phys. Fluids **B5**, 590 (1993)

[12] J. Garnier, Phys. Plas. **6**, 1601 (1999)

[13] S. N. Dixit, M. D. Feit, M. D. Perry and H. T. Powell, Optics. Lett. **21**, 1715 (1996)

[14] J. S. Liu and M. R. Taghizadeh, Optics Lett. **27**, 1463 (2002)

[15] P. Wegner unpublished, private communication (1997)

[16] H. A. Rose and D. F. Dubois, Phys. Rev. Lett. **72**, 2883 (1994)

[17] Ph. Mounaix, L. Divol, S. Huller and V. T. Tikhonchuk, Phys. Rev. Lett. **85**, 4526 (2000)

[18] Ph. Mounaix, Phys. Rev. Lett. **87**, 085006 (2001)

[19] L. Divol, private communication (2005)

[20] B. Ya Zeldovich, N. F. Pilipetsky and V. V. Shkunov *Principles of Phase Conjugation* Springer Verlag (Berlin 1985)

[21] H. A. Rose, Phys. Plas. **2**, 2216 (1995)

[22] H. A. Rose, Phys. Fluids **B5**, 3337 (1993)

[23] A. J. Schmitt and B. B. Afeyan, Phys. Plas.**5**, 503 (1998)

[24] C. H. Still et. al. Phys. Plas. **7**, 2023 (2000)

[25] R. L. Berger et. al. Phys. Fluids **B5**, 2243 (1993)

[26] A. J. Schmitt, Phys. Fluids **31**, 3079 (1988)

[27] E. M. Epperlein, Phys. Rev. Lett. **65**, 2145 (1990)

[28] E. M. Epperlein and R. W. Short, Phys. Fluids **B4** , 2211 (1992)

[29] V. Yu. Bychenkov, W. Rozmus, A. V. Brantov and V. T. Tikhonchuk, Phys. Plas. **7**, 1511 (2000)

[30] R. L. Berger, E. J. Valeo and S. Brunner, Phys. Plas. **12**, 062508 (2005)

[31] H. A. Rose, Phys. Plas. **3**, 1779 (1996)

[32] D. E. Hinkel, E. A. Williams and C. H. Still, **77**, 1298(1996)

[33] S. H. Glenzer et. al. Phys. Rev. Lett. **80**, 2845 (1998)

[34] J. R. Moody et. al. Phys. Rev. Lett. **86**, 2810 (2001)

[35] S. Skupsky, R. W. Short et. al. J. Applied Phys. **66**, 3456 (1989)

[36] E. Lefebvre et. al. Phys. Plas. **5**, 2701 (1998)

[37] D. E. Hinkel et. al. Phys. Plas. **5**, 1887 (1998)